PERGAMON

International Journal of Mechanical Sciences 44 (2002) 703–723

International Journal of MECHANICAL SCIENCES

www.elsevier.com/locate/ijmecsci

A new stress-based model of friction behavior in machining and its significant impact on residual stresses computed by finite element method

Xiaoping Yang[a,*], C. Richard Liu[b]

[a] *Cummins Inc., Mail Code: 91617, 635 South Mapleton, Columbus, IN 47201, USA*
[b] *School of Industrial Engineering, Purdue University, 1287 Grissom Hall, West Lafayette, IN 47907-1287, USA*

Received 26 March 2001; received in revised form 6 November 2001

Abstract

Friction modeling in metal cutting has been recognized as one of the most important and challenging tasks facing researchers engaged in modeling of machining operations. To address this issue from the perspective of predicting machining induced residual stresses, a new stress-based polynomial model of friction behavior in machining is proposed. The feasibility of this methodology is demonstrated by performing finite element analyses. A sensitivity study is performed by comparing the cutting force and residual stress predicted based on this new model with those based on a model using an average coefficient of friction deduced from cutting forces and a model using an average coefficient of friction deduced from stresses. The average coefficient of friction computed based on the measured cutting forces is the conventional approach and is still widely used. The average coefficient of friction due to stresses can be considered as a simplified version of the proposed model. Simulation results show significant difference among the predicted residual stresses. As the proposed model is able to capture the relationship between the normal stress and shear stress on the tool rake face better than the conventional approach can, it has a potential for improving the quality of the prediction of the residual stresses induced by machining. © 2002 Elsevier Science Ltd. All rights reserved.

Keywords: Friction modeling; Residual stress; Finite element; Metal cutting

1. Introduction

1.1. Motivation

It is conceivable that enhancing product competitiveness is of paramount importance for a company to excel. For the design and manufacturing of fatigue critical products, such as aircraft, nuclear

* Corresponding author.
E-mail addresses: xiaoping.yang@cummins.com (X. Yang), liuch@ecn.purdue.edu (C.R. Liu).

PII: S0020-7403(02)00008-5

Nomenclature

A	apparent area of contact
A_r	real area of contact
N	normal load
B	constant
σ	normal stress on tool rake face
τ	friction shear stress on tool rake face
τ_{crit}	critical shear stress
$\bar{\tau}_{\max}$	maximum shear stress
μ	friction coefficient
F_c	cutting force
F_t	thrust force
α	tool rake angle
c	coefficient
λ	characteristic constant
τ_t	frictional stresses
σ_t	normal stress
k	principal shear stress of chip surface layer in contact with tool-face
τ_f	frictional stress
H_v	Vickers hardness
p	contact pressure expressed in MPa
a_n	coefficients
n	increment number
D	material parameter
p	material parameter
σ	effective yield stress at a nonzero strain rate
σ_0	static yield stress
$\dot{\bar{\varepsilon}}^{\mathrm{pl}}$	equivalent plastic strain rate

power plants, and automobiles, understanding and controlling the variance of fatigue life are essential to achieve this goal since fatigue is their predominant mode of failure. An important way to understand the variance of fatigue life is to build models capable of predicting this information accurately [1]. Previous studies have shown the dominant role of residual stress in dictating both the variance and average value of fatigue life [2–7]. Hence, obtaining correct residual stress information is a prerequisite for accurate prediction of fatigue life. Currently, the determination of residual stress heavily depends on experimentation. However, experimental approach has many limitations, for example:

- time consuming and labor intensive;
- sample size and sample shape that can be measured are limited;

- has difficulties accessing some key locations on the part;
- accuracy of measurement depends on operator skill and machine capacity.

Therefore, developing a methodology capable of accurately predicting machining induced residual stress is of great value. As it has been shown that the prediction of machining induced residual stress is sensitive to the coefficient of friction [8], this paper further addresses friction modeling from the perspective of residual stress prediction.

Friction modeling in metal cutting has been recognized as one of the most important and challenging tasks facing researchers engaged in modeling of machining operations [9]. In the following subsections, research on this issue is reviewed first, and then a stress-based polynomial friction model is proposed and its impact on the prediction of residual stresses evaluated.

1.2. Classical models

It has been recognized in early years of metal cutting research that coefficients of friction obtained in metal cutting are often greatly different from those obtained with the same metal pair in conventional sliding-friction experiments [10–12]. Under usual conditions where the real area of contact A_r is only a small percentage of the apparent area of contact A ($A_r \ll A$), Amontons's [13] rules represent good approximations for clean, dry, smooth surfaces sliding in air:

1. The coefficient of friction is independent of applied load N.
2. The coefficient of friction is independent of apparent area of contact A.

However, in the case of metal cutting, the contact pair on the tool chip interface is under extreme conditions where the ratio A_r/A is increased and usually reaches 1. The Amontons's rules fail to capture the relationship between normal force and shear force. Finnie and Shaw [10] proposed an exponential relationship linking the real area of contact with the apparent area of contact in metal cutting:

$$\frac{A_r}{A} = 1 - e^{-BN}, \tag{1}$$

where A is the real area of contact, A is the apparent area of contact, B is a constant, and N is the normal force (Fig. 1). The curve for normal stress and shear stress is similar to that of Fig. 1. Later, Shaw et al. [14] studied friction characteristics of sliding surfaces undergoing subsurface plastic flow. The curve fitted from their experimental data for the relationship between normal stress and shear stress resembled that of Fig. 1.

Zorev [12] proposed the distribution of shear and normal stresses on rake face of tool as shown in Fig. 2. The contact area on the tool rake face is divided into two parts: sticking region (AB) and sliding region (BC). In the sticking region, the shear stress is believed to be equal to the shear strength of the material being machined; in the sliding region, the coefficient of friction is believed to be independent of normal stress. This model has been widely cited and used, for example, Ref. [15]. Wallace and Boothroyd [16] also obtained similar results and concluded that the coefficient of friction is constant in sliding region.

The use of average coefficient of friction as computed from cutting forces has long been criticized [10,11]. It has been suggested that the use of the misleading average coefficient of friction

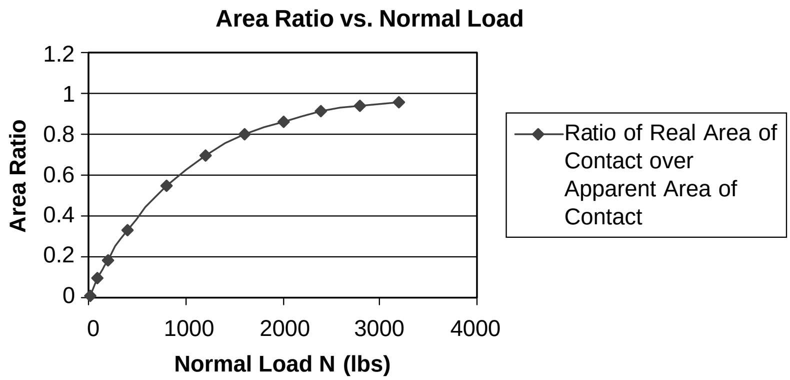

Fig. 1. Ratio of real area of contact over apparent area of contact versus normal load in metal cutting (after Ref. [10]).

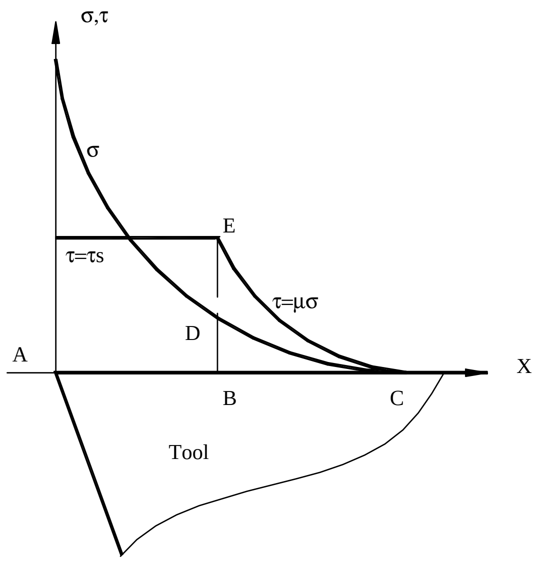

Fig. 2. Zoerv's rake face normal and shear stress distribution model (after Ref. [12]).

be suspended. Fenton and Oxley [17] replaced it with the average shear stress along tool–chip interface.

Moufki et al. [18] proposed a temperature-dependent friction modeling of metal cutting. Their model depended on a shear angle solution, an estimation of the interface temperature, and an estimation of pressure distribution on the rake face. They have compared their predicted value of mean coefficients of friction with those deduced from cutting forces.

1.3. Modeling of friction in computational analyses of metal cutting

There are several approaches to model friction in finite element simulation of metal cutting. Coulomb's law of friction was used by Strenkowski and Moon [19] ($\mu = 0.2$) and Lin and Lo [20]

($\mu = 0.1$). Zorev's sticking-sliding friction model was another approach and was widely used with some variations. In Ref. [21] ($\mu = 0.14$) and Refs. [22,23], the length of each region is either prescribed or assumed. In Refs. [8,24–26], the following criteria are used and the programs automatically determine the slide region and sticking region:

$$\tau_{\text{crit}} = \mu\sigma \quad \text{when } \tau < \bar{\tau}_{\max}, \tag{2a}$$

$$\tau = \bar{\tau}_{\max} \quad \text{when } \tau \geqslant \bar{\tau}_{\max}. \tag{2b}$$

While the first three papers chose their coefficient of friction without verification, the last five papers adjusted the selection of friction coefficient by the simulation results. In Oh and Warnecke's [26] verification, the effect of temperature on the frictional behavior was taken into consideration. In addition to the μ, they also adjusted $\tau_{\max}$. In Refs. [8,23–25] the measured cutting forces were used. For instance, in Ref. [8], in the case of sharp tool, the mean coefficient of friction between tool and chip in orthogonal cutting was calculated by

$$\mu = c\frac{F_{\text{t}} + F_{\text{c}}\tan\alpha}{F_{\text{c}} - F_{\text{t}}\tan\alpha}, \tag{3}$$

where F_{c} and F_{t} were measured cutting and thrust forces, α was rake angle, and c was a coefficient. If the difference was $< 5\%$, the friction coefficient was considered acceptable.

Usui and Shirakashi [27] derived a stress characteristic equation of the tool-face friction from Eq. (1):

$$\tau_{\text{t}} = k(1 - \mathrm{e}^{-\lambda\sigma_{\text{t}}/k}), \tag{4}$$

where λ is the characteristic constant, τ_{t} and σ_{t} are frictional and normal stresses, respectively, and k is the principal shear stress of chip surface layer in contact with tool-face. They fitted experimental value of σ_{t} and τ_{t} on tool rake face obtained by using a split tool to Eq. (4). The reported materials tested were α-brass, pure aluminum, and S15C steel.

Recognizing that a difference between friction in cutting and friction under conventional conditions is that newly created surface directly contacts the tool surface, Iwata et al. [28] proposed a method to test friction between new surfaces and a tool material. Based on experimental results, they proposed the following relationship:

$$\tau_f = \left(\frac{H_{\text{v}}}{0.07}\right)\tanh\left(\frac{0.07\mu p}{H_{\text{v}}}\right) \text{ MPa}, \tag{5}$$

where μ was the coefficient of friction in low pressure range, H_{v} was the Vickers hardness of the workpiece material, and p is the contact pressure expressed in MPa. They had to introduce a frictional shear factor into this relationship in order to make the computed results agree with those of experiment. Their predicted cutting force, the cutting ratio, and the contact length agreed with the experimental ones. The predicted thrust force was lower than experimental one due to the approximation nature of the friction model. The radius of chip curl was easily influenced by the friction condition and thus only a qualitative agreement was seen.

1.4. Study on the sensitivity of residual stress to the coefficient of friction

Liu and Guo [8] have studied the residual stress sensitivity to friction condition of tool–chip interface. Their friction model is based on a single average friction coefficient. Three coefficients of friction are studied: 0.3, 0.5, and 0.7. As the friction value increases from 0.3 to 0.5, and then to 0.7, residual stress changes from tensile to compressive on the machined surface. The residual stress distribution pattern changes correspondingly.

1.5. A stress-based polynomial model of friction behavior in machining

The core function of a friction coefficient is to link normal force with shear force of a contact pair. It can also be expressed by a relationship linking normal stress with shear stress of a contact pair, which is useful when distribution of forces varies significantly such as in metal cutting. Under conditions where Coulomb's law of friction is obeyed, a single coefficient is sufficient to describe the relationship between the normal force and shear force of a contact pair. Under extreme conditions such as those on the rake face in metal cutting, a single coefficient of friction is no longer able to represent the relationship between normal force and shear force. In current practice, an average coefficient of friction relating average force to average shear force has been used. Meanwhile, it has been criticized for being misleading. Suggestions have been made that its use be suspended. Nevertheless, the use of average coefficient of friction in metal cutting continues due to its simplicity and the fact that no proper form has been discovered.

As an attempt to model the complex friction behavior in machining, the following equation is proposed to represent the most general relationship between normal stress and shear stress:

$$\tau = f(\sigma). \tag{6}$$

Eq. (6) may be reduced to Eq. (2) when Coulomb friction holds. It may also take the form of Eq. (4) or (5), as long as they capture the true relationship between the normal stress and shear stress.

Due to the versatility of polynomials, we further propose a special form of Eq. (6) that can represent the relationship between shear stress and normal stress under most cases:

$$\tau = \sum_{n=0}^{n=4} a_n \sigma^n. \tag{7}$$

When $a_n = 0$ for $n = 0, 2, 3, 4$, Eq. (7) is reduced to Eq. (2a). When $a_n = 0$ for $n = 1, 2, 3, 4$, Eq. (7) is reduced to Eq. (2b) and $a_0 = \tau_{\max}$. The n can also be larger than 4 if it is justified by the circumstance.

This relationship is important for computer simulation of a metal cutting process. The current state-of-art in finite element analysis is such that the program can compute the normal stresses given the cutting conditions but not shear stresses without this relationship. As computer simulation is recognized as an indispensable tool to metal cutting research [9], the significance of this relationship goes beyond computer simulation itself.

How to find the polynomial coefficients for Eq. (7) is the key question of this approach. Any attempt falling short of capturing the true state on the tool–chip interface with extreme conditions of pressures and temperatures, chemical and physical reactions between the partners involved (tool, chip, and possibly cutting fluid) is unlikely to capture the true relationship between normal stress and shear stress on the tool rake face [9]. Therefore, the best way to capture the true relationship between normal and shear stresses on rake face is to measure the normal and shear stresses during actual metal cutting processes. There are two techniques measuring these stresses during metal cutting: photoelastic method and split tool. Section 2 reviews research results regarding tool rake face stress distributions in metal cutting using photoelastic technique and split-tool technique. It is an open question how accurate these techniques can capture the stress state on the tool rake face. This paper discusses a hypothetical case assuming an experimental tool rake face σ–τ relationship obtained from the split-tool technique is true to the proposed computational models. Section 3 demonstrates the feasibility of the proposed polynomial friction model using this relationship from Section 2. As a comparison, residual stresses are also predicted by finite element model using the average friction coefficient deduced from cutting forces and the average friction coefficient deduced from shear and normal stresses in the sliding region (BC in Fig. 2). The first average coefficient of friction is called force-based coefficient. It is used as a comparing basis due to its wide applications. The second coefficient of friction is called stress-based coefficient. It is used to evaluate the necessity of effect of treating the coefficient of friction as a constant vs. as a variable. It is treated as a constant in Zorev's model. It is believed that the coefficient of friction is constant in sliding region [15]. When come to finite element modeling, it is also treated as a constant [8,21–26]. However, a closer look at Fig. 2 reveals this may not be true as curve CD and curve CE are not parallel.

It is noted that certain assumptions have to be made to implement the computational models. They are discussed later in Section 3. However, it is emphasized that the objective of this paper is not to obtain the absolute value of the computed quantities. Instead, the goal of this study is to compare the impact of different friction modeling on the computed quantities. As the simplifying assumptions are applied to each friction model the same way, the approximation due to these assumptions is expected to have insignificant impact on the final result.

2. Capturing the true stress state on the tool rake face

The best way to capture the true stress state on the tool rake face in metal cutting is to measure the stress on the rake face during metal cutting using cutting conditions as close to production conditions as possible.

Two commonly used techniques of analyzing the rake face stress distribution in metal cutting are photoelastic method and split tool. Numerous researchers have conducted research applying one of the methods to determine the rake face stress distributions. For example, Rice et al. [29], Usui and Takeyama [30], Chandrasekaran and Kapoor [31], Ramalingam and Lehn [32], Ramalingam [33], and Bagchi and Wright [34] have applied the photoelastic method to study stress distributions on rake face in machining. Kato et al. [35], Barrow et al. [36], and Buryta et al. [37] have applied split tool to study stress distributions on rake face in machining.

Fig. 3 reproduces the curve types of typical experimental results on tool–chip interface stress distributions after Ref. [38]. There are three types of shear stress distribution and four types of normal stress distribution. Table 1 summarizes some of previous research on rake face stress distribution including method of stress determination, materials studied, and cutting tool and conditions, and

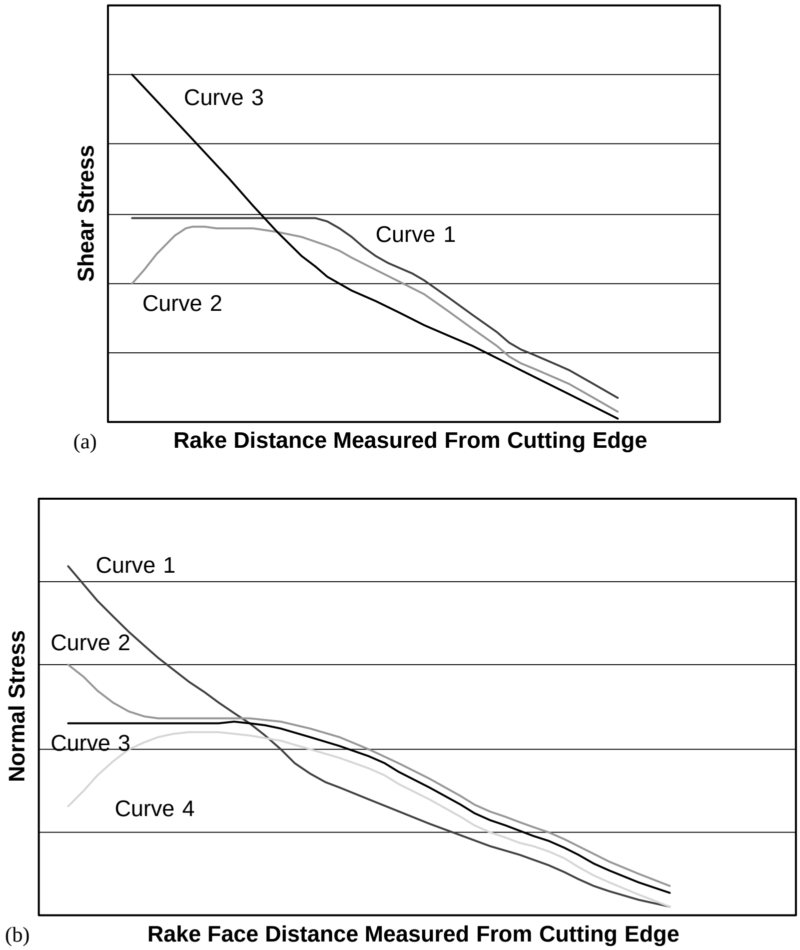

Fig. 3. Typical experimental stress distributions: (a) shear stress; and (b) normal stress (after Ref. [38]).

curve type. (The curve-type number refers to the curve-type number as shown in Fig. 3.) The general trend of the study is to move from easy-to-cut materials such as lead at low speed to materials and cutting conditions more representative of real applications. Due to the limitations of photoelastic materials strength, early investigations applying photoelastic method often cut lead at very low speed, for instance, 25.4 mm/min in Ref. [31]. Bagchi and Wright [34] used transparent single crystals of sapphire and were able to cut brass and steels up to 60 and 75 m/min. The materials used for making split-tool are stronger. In an early study by Kato et al. [35], materials cut included aluminum, copper, zinc, and lead–tin alloy at 50 m/min. In a more recent study by Buryta et al. [37], steels were cut at 130 m/min. Split-tool technique was criticized for not having adequate resolution in the immediate vicinity of the cutting edge [34].

Although there are limitations to both photoelastic and split-tool techniques, useful information can be obtained from applying them to study the rake face stress distributions. The most valuable information is the one gained from cutting conditions representative of real applications. Yet so far,

Table 1
Some previous results on tool rake face stress distribution

Researcher(s)	Method of stress determination	Material(s) studied	Cutting tool and conditions	Stress distribution	
				Shear	Normal
Rice et al. [29]	Photoelastic	Lead	Catalin 61-893, 50° isoclinics, 17.5° rake, 0.01 in DOC, 10 fpm max speed	No data	Fig. 3(b), curve 2
Usui and Takeyama [30]	Photoelastic	Lead	Epoxy resin, 40° isoclinic line, 7° rake, 0.2 in WOC, 0.0342 in DOC, 0.71 ipm speed, dry cutting.	Fig. 3(a), curve 1	Fig. 3(b), curve 2
Chandrasekaran and Kapoor [31]	Photoelastic	Lead	VP-1527, −10°, 0°, 10°, 20° rake, 10° clearance, 10 mm WOC, 0.75 mm DOC, 25.4 mm/min speed, dry cutting	Fig. 3(a), curve 2 for −10° rake, curve 1 for other rakes	Fig. 3(b), curve 1 for 0° rake, curve 3 for other rakes
Kato et al. [35]	Split tool	Aluminum (hardened and annealed), copper (half hardened), zinc, and lead–tin alloy.	HSS, 0°, 10°, 20° rake, 7° relief, 5, 10 mm WOC, 0.1, 0.2, 0.3 mm DOC, 50 m/min speed, 300 mm LOC, dry cutting	Fig. 3(a), curve 3 for Zn with 20° rake, Fig. 1(a), curve 1 otherwise	Fig. 3(b), curve 1 for Zn, Fig. 1(b) curve 3 otherwise
Bagchi and Wright [34]	Photoelastic	12L14 steel, 1020 steel, and 360 brass	Sapphire, −5° rake, 5° clearance, 15° isoclinics, 10, 25, 60, and 75 m/min speed 0.132 mm/rev and 0.381 mm/rev feed.	Fig. 3(a), curve 2	Fig. 3(b), curve 1
Barrow et al. [36]	Split tool	Nickel–chromium steel	Carbide tool, cutting speeds at 30, 45, 60, 120 m/min, DOC 90, at 0.356 mm, 0.254 mm, 0.160 mm, dry cutting	Fig. 3(a), curve 1	Fig. 3(b), curve 3
Buryta et al. [37]	Split tool	AISI C1045, AISI 304, SAE CA 360	K68 from Kennametal, −5° rake, 5° clearance, speed, 130 m/min 0.152 mm/rev feed, dry cutting.	Fig. 3(a), curve 1 after fitting the data to match most published results	Fig. 3(b), curve 3

many friction models in metal cutting seem to be oblivion to this information. Most papers studying rake face stress distributions in literature were focusing on determining the general pattern of normal stress and shear stress [34–37] and did not link quantitatively the shear stress and normal stress on the tool rake face. Usui and Shirakashi [27] applied rake face stress distributions from split-tool test to justify the proposed Eq. (4). However, their model was based on the assumption that σ–τ relationship on the tool rake face followed an exponential one similar to that shown in Fig. 1 with

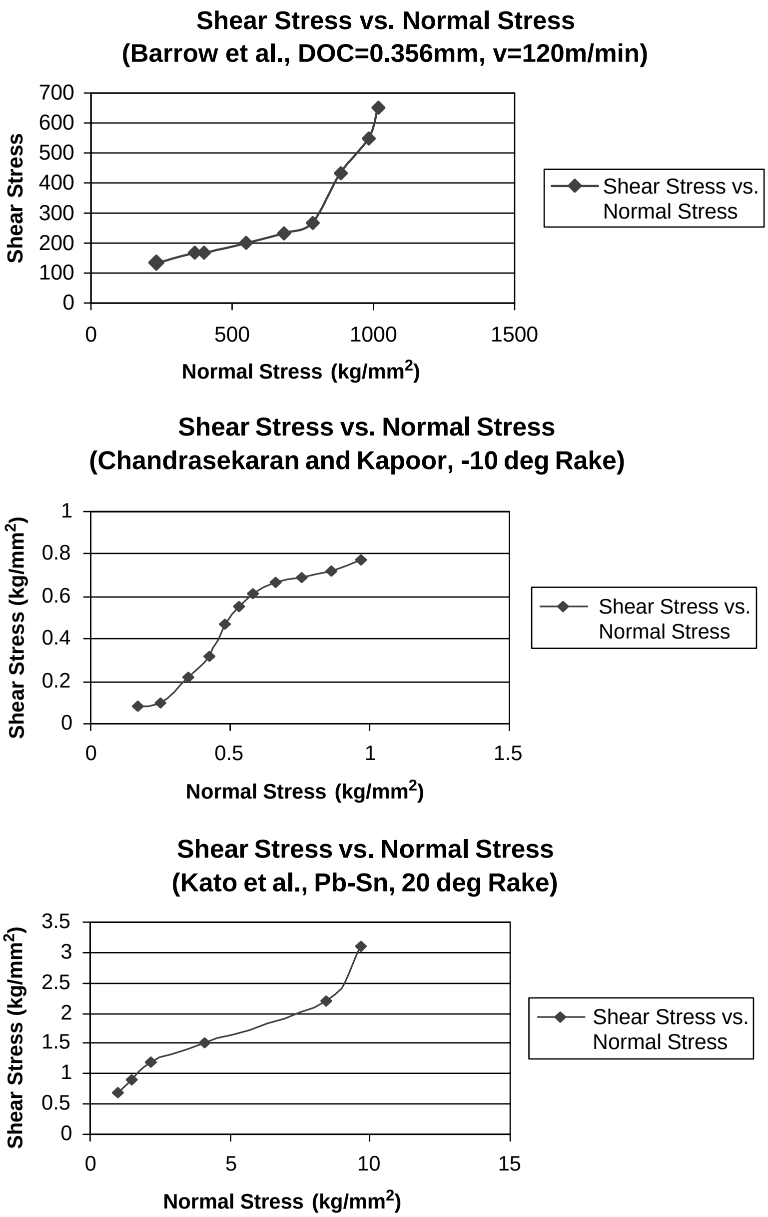

Fig. 4. σ–τ relationship on tool rake face in metal cutting from three previous papers.

the load being replaced by normal stress and area ratio being replaced by shear stress. The scope of their split-tool test was very limited. Whether this type of function can capture the true relationship between the normal stress and shear stress on rake face in metal cutting in general is scrutinized.

Fig. 4 shows three σ–τ relationship curves produced from the results of three previous papers: Barrow et al. [36] that used split-tool technique, Chandrasekaran and Kapoor [31] that used photoelastic technique, and Kato et al. [35] that used split-tool technique. Just as the friction coefficient for different contact pairs may be different under conventional conditions, the σ–τ relationship curve for different cutting tool material/workpiece material pair and cutting conditions may be different.

Assuming that these experimental data are accurate, it is clear that new functions other than an exponential one is needed to represent the σ–τ relationship curve on tool rake face.

3. Computational friction modeling in metal cutting—a polynomial approach

In the introduction, we propose Eq. (7), a polynomial to represent the σ–τ relationship on the tool rake face. In Section 2, we present some experimental data from which the coefficients of polynomial in Eq. (7) can be computed. In this section, a polynomial is determined for the first curve in Fig. 4 (after Ref. [36]) assuming it is the accurate σ–τ relationship on tool rake face for the machining parameters and material properties defined in Tables 2 and 3. A finite element model is then built based on the proposed polynomial friction models. The paper of Barrow et al. [36] is selected because their tests were performed under a range of realistic cutting conditions. Among their data, the most reliable one was the set at high cutting speed (120 m/min) and high depth of cut (0.356 mm), which is the basis for drawing the first curve of Fig. 4. It is interesting to note the difference between this curve and the curves in Figs. 1 and 2. Why the shear stress grows that way is unknown. The different experimental conditions may have led to the different curve trend.

Two models using average friction coefficients, one from cutting force and one from rake face stress distributions are also built. Comparisons are made of predicted values including cutting force and residual stress among the three models.

3.1. Finite element modeling and assumptions

A commercial finite element software ABAQUS/Explicit [39] is used to model the metal cutting process. This selection is based on the following reasons: the explicit dynamic method was originally developed to analyze high-speed dynamic events that are extremely costly to analyze using implicit programs, such as ABAQUS/Standard. The explicit dynamic method also has advantages over the implicit method in modeling complex contact problems and materials with degradation and failure, which is essential to model a metal cutting process.

The element used to model the workpiece is a four-node bilinear plane strain element CPE4R. This is acceptable as in many cases the width of cut is at least five times the depth of cut and the chip is produced in plain strain [40]. The CPE4R comes with hourglass control that is important in dealing with large deformation during metal cutting. The bottom element of the workpiece is restrained from moving in both directions 1 and 2.

Table 2
The cutting tool geometry and cutting conditions

Rake angle	30°
Clearance angle	5°
Cutting speed	2 m/s
Depth of cut	0.356 mm
Initial temperature	25°

Table 3
The thermo-elastic–plastic material properties of 304 stainless steel (after Ref. [8])

Density	7800 kg/m^3
Strain-rate dependent	$D = 1500,\ p = 6$
Inelastic heat fraction	0.6
Specific heat (J/kg, $^\circ$C)	(450, 25)
	(500, 100)
	(525, 450)
	(550, 850)
Poisson's ratio	(0.3, 25)
	(0.3, 260)
	(0.28, 480)
	(0.28, 700)
Young's modulus (GPa, $^\circ$C)	(193, 25)
	(179, 260)
	(160, 480)
	(140, 700)
Yield and fracture strength, fracture strain, and temperature (MPa, $^\circ$C)	(230, 0, 25)
	(554, 1.6, 25)
	(154, 0, 426)
	(430, 1.19, 426)
	(146, 0, 537)
	(390, 1.35, 537)
	(96, 0, 648)
	(289, 0.77, 648)

The tool is modeled as a perfectly rigid body because most tool materials have significantly high elastic moduli. Compared with the large plastic deformation of workpiece, the elastic deflection of the cutting tool can be ignored. The boundary conditions are such that the tool can move freely in direction 1 while its other degrees of freedom are restrained.

Fig. 5 shows the finite element modeling of the cutting process.

Other assumptions for the model include that the chip formation is continuous, the workpiece is stress free prior to the cutting operation, and that cutting tool wear and residual stress from phase transformation are ignored.

Table 2 shows the cutting tool geometry and cutting conditions.

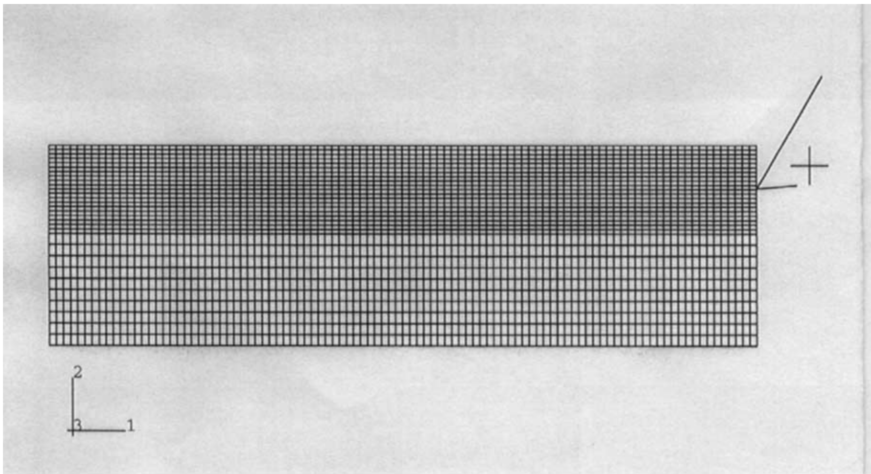

(a)

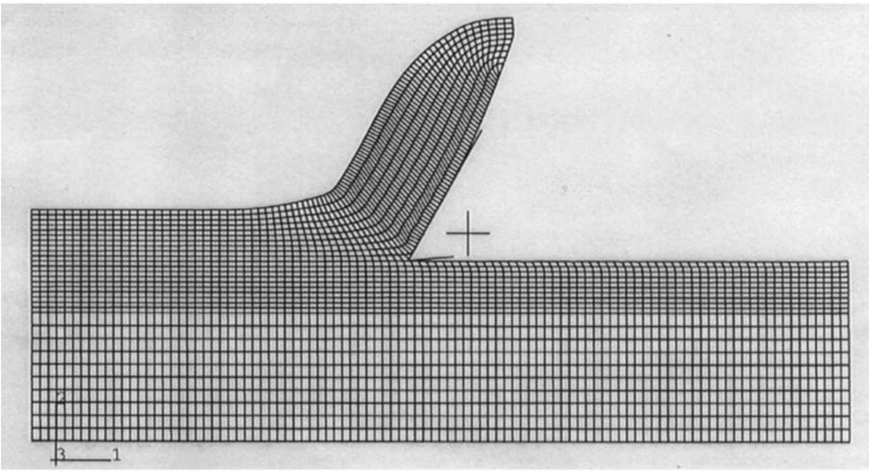

(b)

Fig. 5. The finite element modeling of a cutting process: (a) before the cutting; and (b) after the cutting.

3.2. Workpiece material, its properties, and finite element modeling

The workpiece material is 304 stainless steel. Table 3 shows thermo-elastic-plastic material properties [8]. This material is not exactly the same material used by Barrow et al. [36], however, they belong to the same class of material.

Due to the large plastic deformation to which the workpiece material is subject in metal cutting process, workpiece material strain hardens. The isotropic hardening model is employed to model this behavior by defining flow stresses as a function of plastic strain and temperature as shown in Table 3.

Another feature of metal cutting is the high strain rate to which the workpiece material is subject. This behavior is modeled by the rate-dependent option in ABAQUS. This option uses the following over stress power law [39]:

$$\dot{\bar{\varepsilon}}^{\mathrm{pl}} = D\left(\frac{\bar{\sigma}}{\sigma_0} - 1\right)^p \quad \text{for } \bar{\sigma} \geqslant \sigma_0, \tag{8}$$

where $\dot{\bar{\varepsilon}}^{\mathrm{pl}}$ is the equivalent plastic strain rate, $\bar{\sigma}$ is the effective yield stress at a nonzero strain rate, σ_0 is the static yield stress, and D, p are material parameters that may be functions of temperature and represent the strain rate sensitivity of the material. In this study, D and p are taken from Ref. [8] and are shown in Table 3.

The heat generation in this study assumes adiabatic condition [8]. As about 90% of the plastic work is converted to heat and about 60–70% of the heat generated goes into chip [41], an inelastic heat fraction of 0.6 is selected (Table 3).

A material ductile failure model based on effective plastic strain is used in this study [8]. When the effective strain of the material reaches the critical value, the material fails. ABAQUS uses von Mises flow criterion to model the material inelasticity. Because of the unusually high stress involved in metal cutting, there is considerable evidence that the transport of disconnected microcracks is involved along with dislocations in steady-state chip formation. Therefore, the von Mises criterion only yields an approximation. However, as the same criterion is applied to all computation regardless of the friction modeling and the objective of this paper is to evaluate the impact of different friction modeling on induced residual stress, this approximation is not expected to have a significant impact on the final comparison.

3.3. Friction modeling

There are three friction models studied: a polynomial σ–τ relationship, an average coefficient of friction based on tool rake face stress distributions, an average coefficient of friction based on cutting forces. The normal stress on tool rake face is computed automatically by letting tool cut the workpiece. The computation of the shear stress is discussed below. The unit for shear stress and normal stress in the following equations is MPa.

3.3.1. Using stress-based polynomial model

A polynomial is fitted to the first curve in Fig. 4. There was no experimental data available for $\sigma < 262$ MPa. It is assumed that in that region, Coulomb's law of friction holds and the coefficient of friction for $\sigma = 262$ is used. The experimental data also showed that the shear stress has a maximum value of 655 MPa. Although $\mathrm{d}\tau/\mathrm{d}\sigma$ is not zero at this point, it is assumed that this is the largest τ value. The justification of this assumption is that physically there is a limit on material shear strength. The observed maximum value serves as a good reference. This paper's objective of comparing the impact of friction modeling on induced residual stress among three models is achieved by applying this same value to all three friction models:

$$\tau = \begin{cases} 655 & \text{if } \sigma \geqslant 1016, \\ 9.52455E\text{-}10\sigma^4 + 6.19696E\text{-}7\sigma^3 & \\ \quad -2.51946E\text{-}3\sigma^2 + 1.71788\sigma - 175 & \text{if } 262 \leqslant \sigma < 1016, \\ 0.45\sigma, & \text{if } \sigma < 262. \end{cases} \tag{9}$$

Table 4
The computation of an average coefficient of friction due to rake face stress distributions

Normal stress (MPa)	Shear stress (MPa)	Coefficient of friction
1016.393	655.7377	0.645161
993.4426	547.541	0.551155
891.8033	422.9508	0.474265
790.1639	262.2951	0.33195
681.9672	236.0656	0.346154
554.0984	200	0.360947
396.7213	167.2131	0.421488
367.2131	167.2131	0.455357
262.2951	118.0328	0.45
Average coefficient of friction		0.448

3.3.2. *Using the average coefficient of friction due to rake face stress distributions (stress-based coefficient of friction)*

As Eq. (9) is complicated, one would ask if there is any merit to it. One way to evaluate it is to compare the simulation results of Eq. (9) with that of an average coefficient of friction due to Eq. (9). The computation of the average coefficient of friction due to rake face stress distributions is shown in Table 4.

$$\tau = \begin{cases} 655, & \text{if } 0.448\sigma > 655, \\ 0.448\sigma. & \end{cases} \tag{10}$$

3.3.3. *Using the average coefficient of friction due to cutting forces (force-based coefficient of friction)*

In many previous researches, cutting forces are used to compute the average coefficient of friction because they are readily available. This study also compares the simulation result using coefficient of friction deduced this way.

When cutting forces are available, the average coefficient of friction can be computed using Eq. (11):

$$\mu = \frac{F_t + F_c \tan \alpha}{F_c - F_t \tan \alpha}. \tag{11}$$

In this study, however, it is computed based on the rake face stress distributions. Barrow et al. [36] concluded that the general pattern of rake face stress distribution takes the form of Fig. 6. The difference between this section and the previous section is as follows:

The average coefficient of friction due to rake face stress distributions is the average value in the region where shear stress goes from C to D while normal stress goes from C to F. On the other hand, cutting forces are the total forces and cannot differentiate between sticking region (AB) and sliding region (BC), the average coefficient of friction is thus the ratio of the area of trapezoid ACDE over that of ACFG.

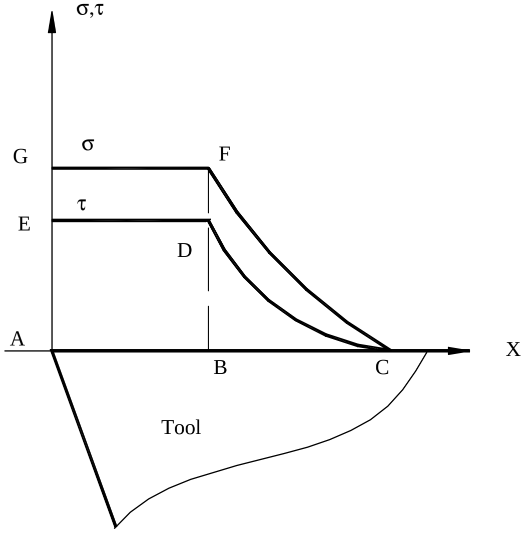

Fig. 6. Barrow et al.'s rake face normal and shear stresses distribution model (after Ref. [36]).

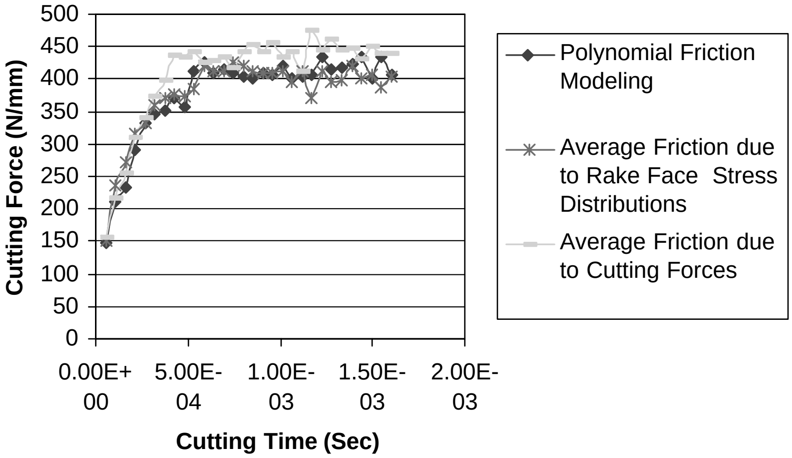

Fig. 7. Simulated cutting forces due to three friction models.

The average coefficient of friction computed in this case is 0.549. The friction modeling is

$$\tau = \begin{cases} 655, & \text{if } 0.549\tau > 655, \\ 0.549\sigma. & \end{cases} \tag{12}$$

3.4. Simulation results

3.4.1. Cutting forces

The simulated cutting forces due to three friction models are shown in Fig. 7. The average cutting forces from 5.33E-4 sec when they begin to stabilize to 16E-3 sec are computed. Using the cutting

Table 5
The average cutting forces due to three friction models

	Polynomial friction model	Average coefficient of friction due to rake face stress distributions	Average coefficient of friction due to cutting forces
Average cutting force (N/mm)	414	406	441
Percentage difference with regard to polynomial friction model	0	−1.9	6.5

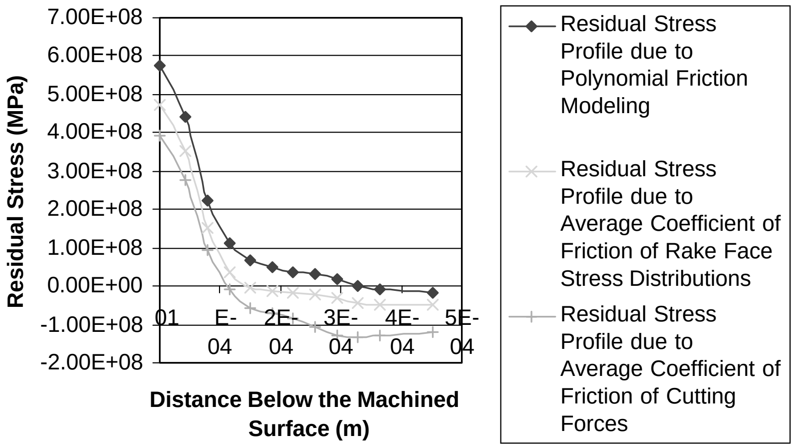

Fig. 8. Simulated residual stress profiles due to three friction models.

Table 6
The maximum residual stress due to three friction models

	Polynomial friction model	Average coefficient of friction due to rake face stress distributions	Average coefficient of friction due to cutting forces
Maximum residual stress (MPa)	575	471	391
Difference with regard to polynomial friction model (absolute/percentage of yield stress)	0	−104/ − 45.2%	−184/ − 80%

forces due to the polynomial friction modeling as a benchmark, the percentage differences due to the other two friction models are also computed. The results are shown in Table 5.

3.4.2. Residual stresses

The in-depth profiles of the simulated residual stresses are shown in Fig. 8. The surface residual stresses are listed in Table 6. Using the residual stress due to the polynomial friction modeling as a benchmark, the differences due to the other two friction models are computed and are also represented in percentage of yield stress of workpiece material at room temperature. The results are shown in Table 6.

4. Discussions

While the polynomial relationship linking shear stress with normal stress in Eq. (9) appears to be daunting, fitting experimental data to this polynomial is straightforward and its computer implementation in finite element friction modeling is feasible.

Although there is no experimental data to verify the simulation results, it is conceivable that correct friction model should capture the true σ–τ relationship on tool rake face. Assuming that curve 1 in Fig. 4 is an accurate σ–τ relationship for the computational model, the polynomial friction model is the best among three models in this study. Using the results from polynomial friction modeling as benchmark, it is seen that the cutting force does not change significantly among the three models (Fig. 7 and Table 5). However, the residual stress result is quite different. Using the stress-based coefficient of friction, the maximum residual stress is about 50% of the yield stress of workpiece material at room temperature less than the benchmark value. Using the force-based coefficient of friction, the maximum residual stress is 80% of the yield stress of workpiece material at room temperature less than the benchmark value.

In both cases, the result of the simulation using the stress-based coefficient of friction is closer to the benchmark value than the simulation using force-based coefficient of friction. The reason is that when cutting force data are used, there is no way to separate the sliding region (BC in Fig. 6) from the sticking region (AB in Fig. 6). As the ratio of shear stress over normal stress is different between sliding region and sticking region, the force-based coefficient of friction distorts the true σ–τ relationship in sliding region. The distortion degrades the simulation results. This is also true in other types of stress distributions on tool rake face, such as the Zorev's model shown in Fig. 2. The magnitude of this distortion depends on the actual stress distributions.

5. Conclusions

1. Yang et al. [5] and Liu and Yang [42] have reported the significant role residual stresses play in determining the fatigue life of a fatigue critical product. Therefore, the accurate prediction of residual stress induced in a machining process is essential for accurate prediction of fatigue life. Liu and Guo [8] have shown that residual stress prediction is sensitive to friction modeling. With a σ–τ relationship hypothetically assumed true for the computational models, this paper investigates the impact of the proposed stress-based polynomial model of friction behavior on the prediction of machining induced residual stress. In order to evaluate the performance of conventional friction modeling methods, the simulation results from the polynomial friction modeling capturing the σ–τ relationship on the tool rake face from the hypothetical case are considered as the benchmark. The difference as large as 80% of the yield stress of workpiece material at room temperature between the benchmark value and the predicted value due to the force-based friction model is observed. This difference shows the inadequacy of the conventional force-based friction model

to predict residual stresses induced in a machining process and the potential of improving the quality in predicting machining induced residual stress by adopting the stress-based polynomial model.
2. As the ratio of shear stress over normal stress on tool rake face in the sliding region may be different from that in the sticking region, the force-based coefficient of friction may distort the true average ratio between shear stress and normal stress in the sliding region. This distortion may further degrade the simulation results. In the case studied, the simulation results from the finite element model using the stress-based coefficient of friction are closer to the benchmark value than are those from the finite element model using the force-based coefficient of friction.
3. Just as the coefficient of friction may be different for different contact pairs in conventional friction tests, the polynomial representing σ–τ relationship on tool rake face may be different for different cutting tool material/workpiece material pairs and cutting conditions.

Acknowledgements

Financial support from NSF award DMI-9900169, with cost sharing from Ford Motor Co., are highly appreciated.

References

[1] Yang Xiaoping. A methodology for predicting the variance of fatigue life incorporating the effects of manufacturing processes. Ph.D. Thesis, Purdue University, 2001.
[2] Koster WP, Field M, Fritz LJ, Luciano RG, Kahles JF. Surface integrity of machined structural components. Technical Report AFML-TR-70-11, Metcut Research Associates Inc., Cincinnati, OH, March, 1970.
[3] Matsumoto Y, Magda D, Hoeppner DW, Kim Tae Young. Effect of machining processes on the fatigue strength of hardened AISI 4340 steel. Journal of Engineering for Industry 1991;113:154–9.
[4] Liu CR, Mittal S. Optimal pre-stressing the surface of a component by superfinish hard turning for maximum fatigue life in rolling contact. Wear 1998;219:128–40.
[5] Yang Xiaoping, Liu CR, Grandt AF. An experimental study on fatigue life variance, residual stress variance, and their correlation of face-turned and ground Ti 6Al-4V samples. Journal of Manufacturing Science and Engineering (ASME), in press.
[6] Yang Xiaoping, Liu CR. The impact of hole making processes on the variance of the fatigue life of the component. Machining Science and Technology, submitted for publication.
[7] Yang Xiaoping, Liu CR. A methodology for predicting the variance of fatigue life incorporating the effects of manufacturing processes. Journal of Manufacturing Science and Engineering (ASME), in press.
[8] Liu CR, Guo YB. Finite element analysis of the effect of sequential cuts and tool–chip friction on residual stresses in a machined layer. International Journal of Mechanical Sciences 2000;42:1069–86.
[9] van Luttervelt CA, Childs THC, Jawahir IS, Klocke F, Venuvinod PK. Present situation and future trends in modeling of machining operations progress report of the CIRP working group 'modeling of machining operations'. Keynote Papers, Presented at the Scientific Technical Committee Paper Discussion Sessions; Annals of the CIRP 1998;47(2):587–626.
[10] Finnie I, Shaw MC. The friction process in metal cutting. Transactions of the ASME 1956;78:1649–57.
[11] Kronenberg M. Machining science and application—theory and practice for operation and development of machining processes. Oxford: Pergamon Press, 1966.
[12] Zorev NN. Interrelationship between shear processes occurring along tool face and on shear plane in metal cutting. In: Shaw MC, editor. International Research in Production Engineering. Proceedings of the International Production Engineering Research Conference, Carnegie Institute of Technology, Pittsburg, PA, 9–12 September, 1963. p. 3–17.

[13] Amontons G. De la Resistance Causeé dans les Machines. Mémories Academie Royale Science 1699:206.
[14] Shaw MC, Ber A, Mamin PA. Friction characteristics of sliding surfaces undergoing subsurface plastic flow. Journal of Basic Engineering 1960;82:342–6.
[15] Shaw MC. Contact problems in cutting and grinding. In: Attia MH, Komanduri R, editors. PED-Vol. 67/Trib-Vol. 4, Contact problems and surface interaction in manufacturing and tribological systems. New York: ASME, 1993. p. 143–9.
[16] Wallace PW, Boothroyd G. Tool forces and tool–chip friction in orthogonal machining. Journal of Mechanical Engineering Science 1964;6(1):74–87.
[17] Fenton RG, Oxley PLB. Mechanics of orthogonal machining: allowing for the effects of strain rate and temperature on tool–chip friction. Proceedings Institution of Mechanical Engineers, Manufacturing and Management Group 1968;183(22 Part 1):417–38.
[18] Moufki A, Molinari A, Dudzinski D. Modeling of orthogonal cutting with a temperature dependent friction law. Journal of the Mechanics and Physics of Solids 1998;46(8):2103–38.
[19] Strenkowski JS, Moon Kyoung-Jin. Finite element prediction of chip geometry and tool/workpiece temperature distributions in orthogonal metal cutting. Journal of Engineering for Industry 1990;112:313–8.
[20] Lin Zone-Chin, Lo Ship-Peng. Ultra-precision orthogonal cutting simulation for oxygen-free high-conductivity copper. Journal of Materials Processing Technology 1997;65:281–91.
[21] Shih AJ. Finite element simulation of orthogonal metal cutting. Journal of Engineering for Industry 1995;117:84–93.
[22] Wu Jung-Shu, Dillon Jr. OW, Lu Wei-Yang. Thermo-viscoplastic modeling of machining process using a mixed finite element. Journal of Manufacturing Science and Engineering 1996;118:470–82.
[23] Shatla M, Yen Y-C, Altan T. Tool–workpiece interface in orthogonal cutting—application of FEM modeling. Transactions of NAMRI/SME 2000;XXVIII:173–8.
[24] Zhang B, Bagchi A. Finite element simulation of chip formation and comparison with machining experiment. Journal of Engineering for Industry 1994;116:289–97.
[25] Guo YB, Liu CR. Residual stress formation mechanism and its control by sequential cuts. North American Manufacturing Research Conference 2000;XXVIII:MR00–199.
[26] Oh Joon-Dong, Warnecke. Mechanically and thermally coupled finite element analysis of chip formation in metal cutting. Transactions of NAMRI/SME 2000;XXVIII:167–72.
[27] Usui E, Shirakashi T. Mechanics of machining-from "descriptive" to "predictive" theory. In: Kops L, Ramalingam S, editors. On the art of cutting metals—75 years later: a tribute to F.W. Taylor. Winter Meeting. Phoenix, AZ: American Society of Mechanical Engineers, 1982. p. 13–35.
[28] Iwata K, Osakada K, Terasaka. Process modeling of orthogonal cutting by the rigid-plastic finite element method. Journal of Engineering Materials and Technology 1984;106:132–8.
[29] Rice WB, Salmon R, Syniuta WD. Photoelastic determination of cutting tool stress. Transactions of the E. I. C 1960;4(1):20–3.
[30] Usui E, Takeyama H. A photoelastic analysis of machining stresses. ASME Journal of Engineering for Industry 1960;82:303–8.
[31] Chandrasekaran H, Kapoor DV. Photoelastic analysis of tool–chip interface stresses. ASME Journal of Engineering for Industry 1965;87:495–502.
[32] Ramalingam S, Lehn LL. A photoelastic study of stress distribution during orthogonal cutting. Journal of Engineering for Industry 1971;93:527–37.
[33] Ramalingam S. A photoelastic study of stress distribution during orthogonal cutting, Part 2: photoplasticity observations. Journal of Engineering for Industry 1971;93:538–44.
[34] Bagchi A, Wright PK. Stress analysis in machining with the use of sapphire tools. Proceedings of the Royal Society of London A 1987;409:99–113.
[35] Kato S, Yamaguchi K, Yamada M. Stress distribution at the interface between tool and chip in machining. ASME Journal of Engineering for Industry 1972;94:683–9.
[36] Barrow G, Graham W, Kurimoto T, Leong YF. Determination of rake face stress distribution in orthogonal machining. International Journal of Mechanical Tools Manufacturing 1982;22(1):75–85.
[37] Buryta D, Sowerby R, Yellowley I. Stress distributions on the rake face during orthogonal machining. International Journal of Mechanical Tools Manufacturing 1994;34(4):721–39.

[38] Arsecularatne JA. On tool–chip interface stress distributions, ploughing force and size effect in machining. International Journal of Mechanical Tools Manufacturing 1997;37(6):885–99.
[39] Hibbitt, Karlsson, Sorensen. ABAQUS/Explicit User's Manual, 1997.
[40] Shaw MC. Metal cutting principles. Oxford: Oxford Science Publications, 1984.
[41] Yang Xiaoping, Liu C Richard. Machining titanium and its alloys. Machining Science and Technology 1999;3(1):107–39.
[42] Liu C, Richard, Yang Xiaoping. The scatter of surface residual stresses produced by face-turning and grinding. Machining Science and Technology 2001;5(1):1–21.